NRIAG Journal of Astronomy and Geophysics (2013) 2, 88–101

National Research Institute of Astronomy and Geophysics

NRIAG Journal of Astronomy and Geophysics

www.elsevier.com/locate/nrjag

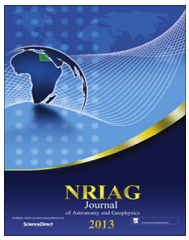

Site-specific shear wave velocity investigation for geotechnical engineering applications using seismic refraction and 2D multi-channel analysis of surface waves

Adel M.E. Mohamed [a,c], A.S.A. Abu El Ata [b], F. Abdel Azim [b], M.A. Taha [a,*]

[a] *National Research Institute of Astronomy and Geophysics (NRIAG), Egypt*
[b] *Faculty of Science, Ain Shams University, Egypt*
[c] *Earthquake Monitoring Center (EMC), Sultan Qaboos University (SQU), Oman*

Received 15 October 2012; accepted 29 April 2013
Available online 1 July 2013

KEYWORDS

Seismic refraction;
1D and 2D MASW;
Geotechnical parameters and Vs^{30}

Abstract In order to quantify the near-surface seismic properties (P- and S-wave velocities, and the dynamic elastic properties) with respect to the depth at a specific area (6th of October club), we conducted a non-invasive and low cost active seismic survey. The primary wave velocity is determined by conducting a P-wave shallow seismic refraction survey. The dispersive characteristics of Rayleigh type surface waves were utilized for imaging the shallow subsurface layers by estimating the 1D (depth) and 2D (depth and surface location) shear wave velocities. The reliability of the Multi-channel Analysis of Surface Waves (MASW) depends on the accurate determination of phase velocities for horizontally traveling fundamental mode Rayleigh waves. Consequently, the elastic properties are evaluated empirically. The Vs^{30} (average shear wave velocity down to 30 m depth), which is obtained from the MASW technique, plays a critical role in evaluating the site response of the upper 30 m depth. The distribution of the obtained values of Vs^{30} through the studied area demonstrates site classes of C and D, according to the NEHRP (National Earthquake Hazard Reduction Program) and IBC (International Building Code) standards.

1. Introduction

In-situ shear wave survey is a geophysical tool of usual practice in earthquake engineering. In traditional engineering surveys, borehole techniques have been considered as standard, due to their relative reliability, even though they are relatively expensive and not suitable for the critical situation of the intensely urbanized settings. Recently, surveys based on surface

* Corresponding author. Tel.: +20 2 25560645.
E-mail address: mohtahan99@yahoo.com (M.A. Taha).
Peer review under responsibility of National Research Institute of Astronomy and Geophysics.

Production and hosting by Elsevier

2090-9977 © 2013 Production and hosting by Elsevier B.V. on behalf of National Research Institute of Astronomy and Geophysics.
http://dx.doi.org/10.1016/j.nrjag.2013.06.012

wave dispersion analysis have been intensively developed, leading to a number of affordable methodologies. These approaches are in fact, free from many practical and theoretical limitations of the body-wave analyses and from the logistic effort of drilling. Surface wave approach is favored by the fact that, Rayleigh and Love waves dominate every seismogram, because of the two-dimensional geometric spreading, that reduces their attenuation with distance and the prevalent generation of surface waves, when using surface sources. Surface wave dispersion is linked to subsoil characteristics, as different frequencies involve different soil thicknesses and consequently travel at different velocities. Dispersion properties can be measured by several procedures, based on phase velocities (e.g. SASW (Nazarian et al., 1983), MASW (Park et al., 1999), REMI (Louie, 2001)) and on group velocities. A further distinction is made between the controlled source surveys and the passive analysis of microtremors and seismic noises (see Zywicki and Rix, 1999).

The site response (transfer function) is evaluated through the geotechnical parameters (layer thicknesses, densities, P-wave velocities, shear wave velocities and damping factor of layers), that are obtained from both the available geotechnical boreholes and the seismic surveys (Mohamed, 2003, 2009; and Mohamed et al., 2008). The P-wave velocity is obtained from the seismic refraction survey and the S-wave velocity is deduced from the Multi-channel Analysis of Surface Waves (MASW) survey.

Prediction of ground shaking response at soil sites requires the knowledge of stiffness of the soil, expressed in terms of shear wave velocity (Vs). This property is useful for evaluating the site amplification (Borcherdt, 1994). The shear wave velocity of each layer of the soil column can be considered as a key element, so the determination of shear wave velocity is a primary task of the current study at the considered area (October 6th club), as shown in Fig. 1.

In Nazarian et al. (1983) have introduced the approach of Spectral Analysis of Surface Waves (SASW), using a two receiver configuration to measure the shear wave velocity and the elastic modulus of soil deposits and pavement. The use of only a pair of receivers leads to the necessity of performing the test using several testing configurations and results in a quite time-consuming procedure in the site for collection of all the necessary data. Subsequently, the method using multiple receivers, called as the Multi-channel Analysis of Surface Wave (MASW), has been proposed and developed to overcome the limitations of the SASW method. The MASW method permits successful identification of different seismic events (body waves backscattered and higher-modes) from the dispersion curve of phase velocity versus frequency plot (Park et al., 1998). In addition, this method also provides a two-dimensional profile of the near-surface that was constructed by combining several one-dimensional shear wave velocity profiles within the uppermost 30 m (Xia et al., 2002). Of all types of seismic waves, the surface waves have the strongest energy with the highest signal-to-noise ratio (S/N) (Park et al., 2002), making it a powerful tool for the near-surface characterization. The MASW is successfully used in many studies (Xia et al., 1999, 2000, 2002; Park et al., 1999; Tian et al., 2003; Kanli et al., 2006; Mahajan et al., 2007; Anbazhagan and Sitharam, 2008).

The P-wave velocity is determined from the shallow seismic refraction survey. Both the P-wave and S-wave velocities are used empirically to evaluate the elastic moduli and geotechnical parameters.

2. Geologic setting

The surface geology in and around the studied area (Fig. 2) reveals that, the oldest rocks are the Upper Cretaceous rocks represented by the Bahariya Formation, the Abu Roash Formation and the Khoman Formation. The Tertiary rocks are represented by the Upper Eocene (Maadi Formation), the Oligocene rocks (Gebel Qatrani Formation and the Basalt flows), the Lower Miocene (Gebel Khashab Formation), the Pliocene (undifferentiated Pliocene deposits) and the Quaternary deposits (Nile deposits). All the investigated sites are occupied by the Gebel Qatrany Formation. This formation is represented by (from the surface geological map and the drilled boreholes) sequence of continental to littoral marine alternating clastics, burrowed siltstone, and reddish claystone.

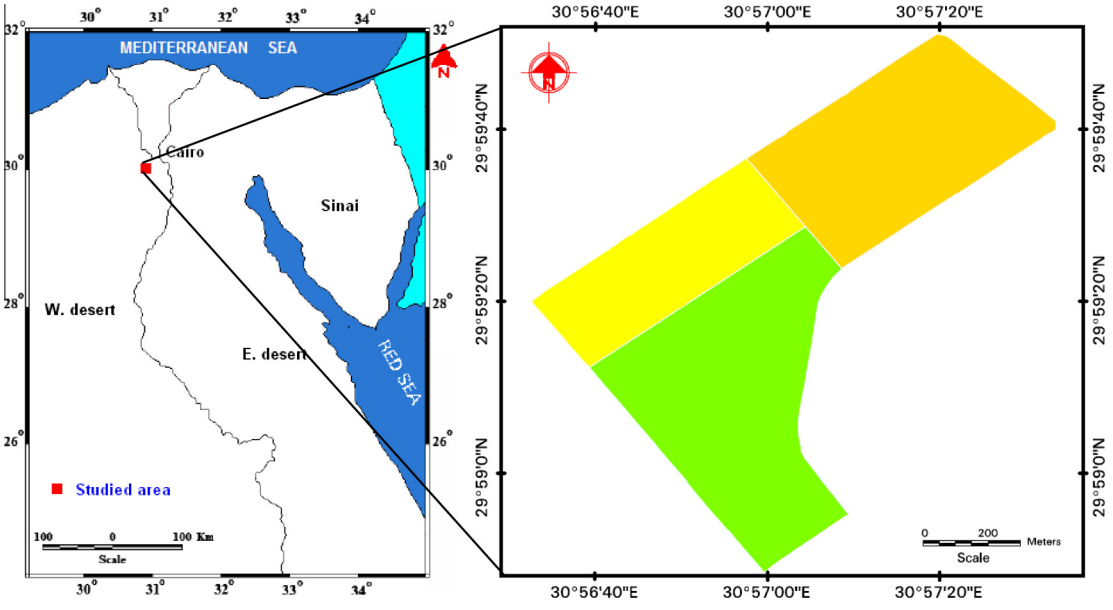

Fig. 1 Location map of the studied area.

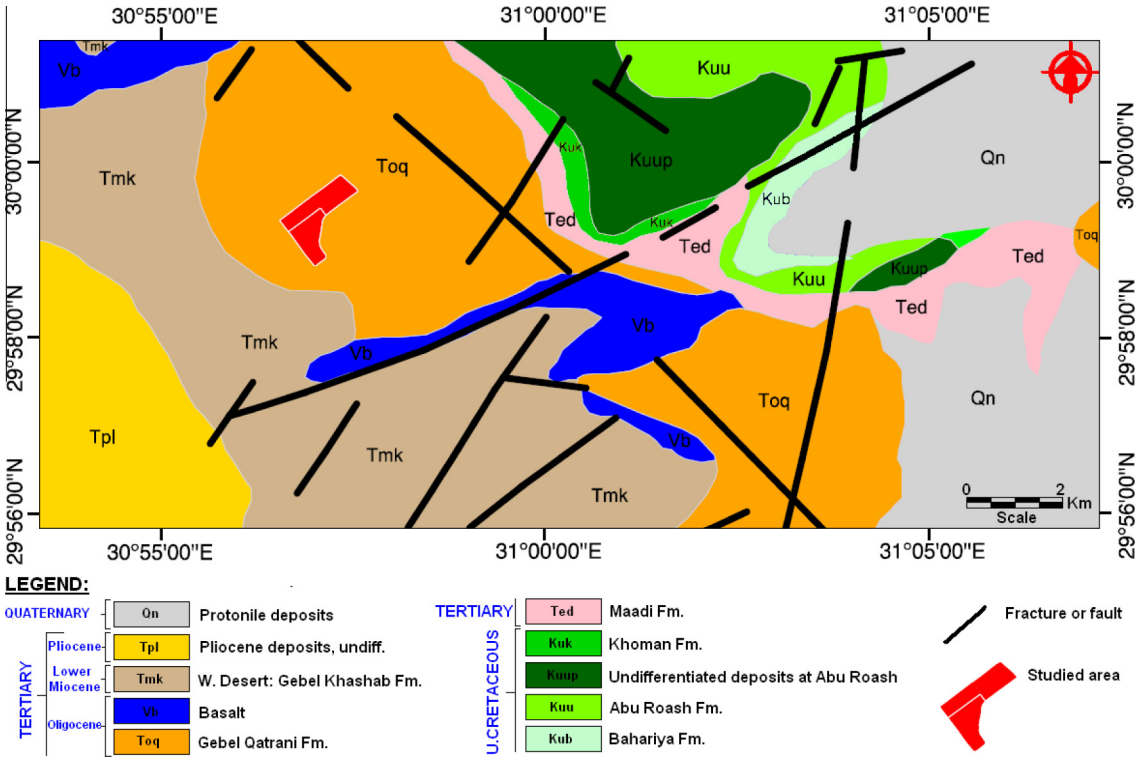

Fig. 2 Geological map of the interested area (modified after Conoco Coral, 1979).

In general, the surface sediment materials in the studied area are loose to a very loose mixture of sand, silt, gravel, clay, and rock fragment material except the top soil layer in some places.

3. Data acquisition

3.1. P-wave seismic refraction

The seismic refraction survey was carried out through applying the forward, inline, midpoint and reverse shootings to create the compressional waves (P-waves). The ground refraction field work is executed in the interested area of the 24 sites (Fig. 3).

The P-waves are acquired by generating seismic energy using an energy source, sending the created seismic waves inside the earth. The direct (head) and refracted (diving) waves are detected through vertical geophones of 40 Hz and recorded using A 48 channel signal enhancement seismograph "StrataView" as data logger. Most of the surveyed 24 profiles have a 94 meter long spread. The geophones, which were firmly coupled to the ground, had 2 m fixed geophone spacing. The technique is to shoot the profile (5 shots) at 5 meters distance from both ends, mid-point, in addition to 2 inline shots (between G12–13 and G36–37). Fig. 4 shows representative P-wave seismograms (five shots) for the seismic profile at site R3C2.

3.2. Multi-channel Analysis of Surface Waves (MASW)

The overall setup of MASW is illustrated in Fig. 5. A 48 channel signal enhancement seismograph "StrataView" of Geometrics Inc., USA, was employed for data acquisition along 24 sites (Fig. 3). Our main task is to estimate the shear wave velocity of the subsurface layers down to at least 30 m, so the frequency content of the records had to be low enough to obtain the phase velocities at longer wavelengths. The lower frequency of signals means that, longer wavelengths of surface waves are recorded, which in turn, results in a larger depth of investigation. Therefore 4.5 Hz geophones, which record the lower frequency components effectively, were used. The recording sampling interval of 1.0 ms and the recording length of 1024 ms were applied. Spread length of 23 m (24 channels) was adopted to use.

The most important parts of the field configurations are the geophone spacing and the offset range. The planar characteristics of surface waves evolve only after a distance greater than the half of the maximum desired wavelength (Stokoe et al., 1994). The acquisition layout was an array of vertical sensors with 1 m geophone spacing and 4 m shot interval. Based upon the field observations, the source to the nearest receiver offset was 5 m to achieve the desired depth probing. The seismic waves were created by the impulsive source of 8 kg (sledge hammer) impact steel plate (of dimensions 200 mm × 200 mm × 50 mm) at least ten shots. Standard roll along technique was used to achieve a continuous shot gather over a line spread of 48 m. This arrangement results in a 2-D section spread over 52 m distance. Fig. 6 shows a typical field configuration. Further details on the MASW and its applications are available in the literature (Xia et al., 1999, 2000 and Park et al., 1999).

4. Data processing

4.1. P-wave seismic refraction

It was pointed out that, the true refractor velocities cannot be determined by shooting at only one end of a seismic line, but such refractor velocities can be determined if the arrival times

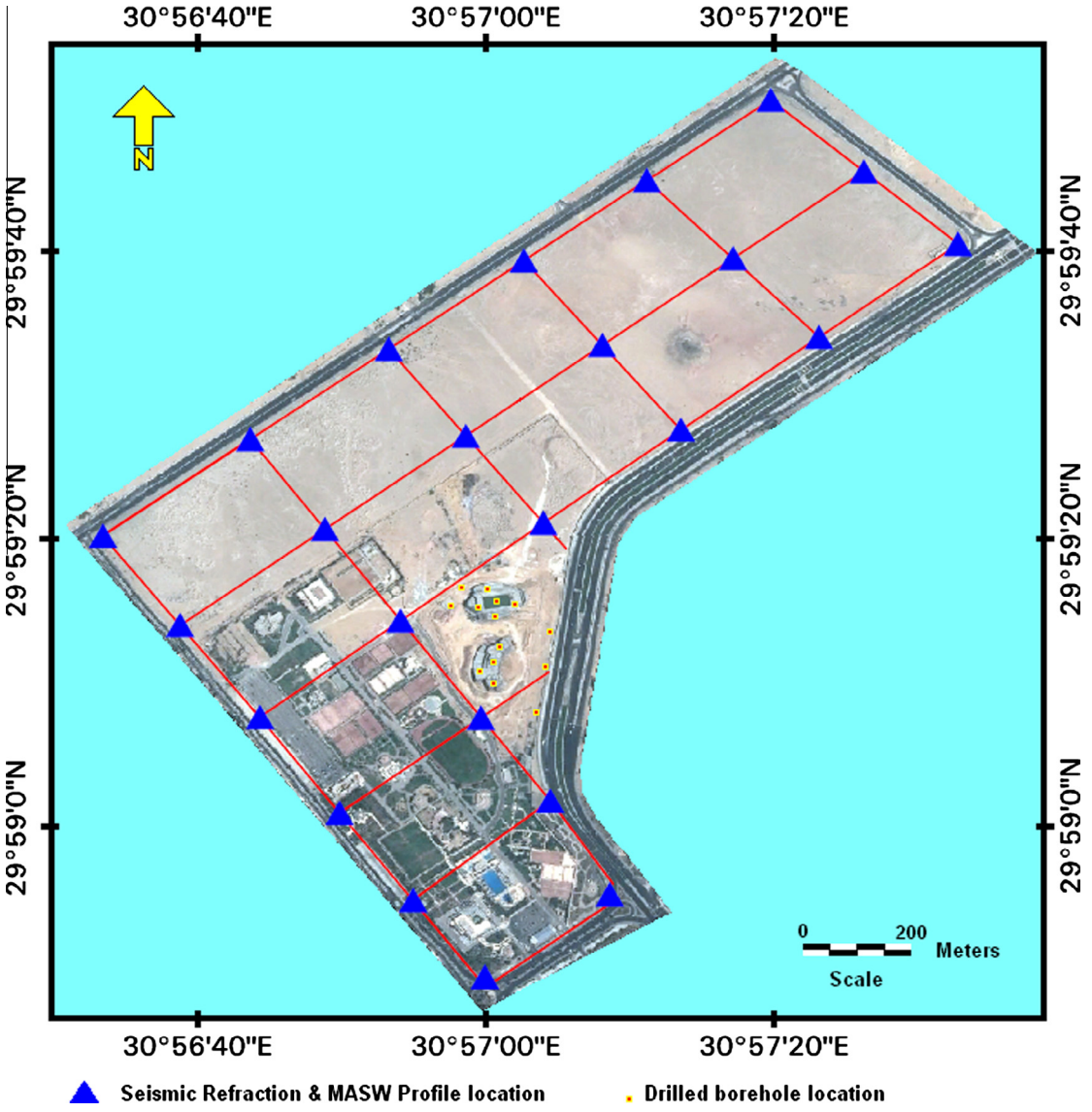

Fig. 3 The location map of the shallow seismic refraction and MASW profiles at the October 6th Club.

are recorded from both ends. Further, a depth computed from an intercept time actually represents the depth of the refracting surface projected back to the shot point. The reversed profile, however, offers a significant advantage in that, the true velocities and thicknesses of the layers can be computed beneath each geophone to allow the mapping of irregular and dipping boundaries by using several methods. The delay-time method was discussed by many authors, as: Gardner (1939), Barthelmes (1946), Slotnick (1950), Tarrant (1956), Wyrobek (1956). The Wave Front method was elaborated by Thornburgh (1930), Gardner et al. (1974), Baumgarte (1955), Hales (1958); and Rockwell (1967). Hagiwara's method was explained by Masuda (1975). The Plus-Minus method was discussed by Hagedoorn (1959) and the Generalized Reciprocal Method (GRM) was introduced by Palmer (1980).

The recorded P-wave data were first corrected to the true elevation of each geophone and then processed and analyzed using the Japanese Code supplied by Oyo (called SeisRefa, 1991). This software uses the ray-tracing and Hagiwara techniques to interactively match the interpreted subsurface model to field data. The wave forms were analyzed by picking the first breaks and determining the travel time-distance (T–D) curves and the comparable depth models (Fig. 7).

4.2. Multi-channel analysis of surface waves (MASW)

The MASW data processing was carried out using "*SurfSeis* 3", which is the software developed in association with rigorous testing of the MASW method developed by the Kansas Geological Survey, USA. Each shot gather consists of 24 channels data. However, the shot gather data require some pre processing precautions. These involve:

(I) The conversion of the raw seismic data format (SEG-2) into Kansas Geological Survey data processing format (KGS or SEG-Y), combining all shot gathers for processing into a single file. Field geometry was assigned and the acquired data were recompiled into the roll-along mode data set.

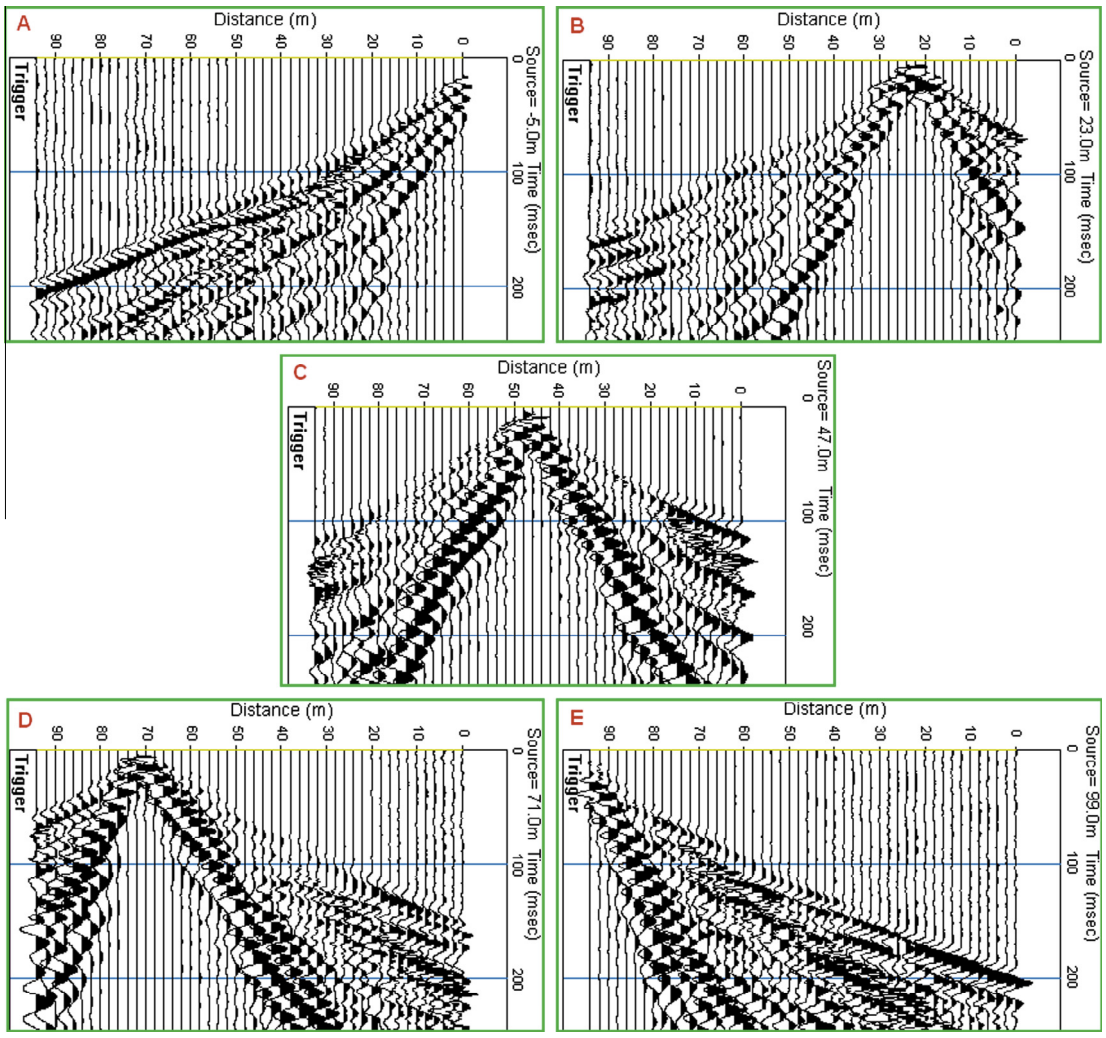

Fig. 4 The P-wave seismograms records at the seismic profile R2C2. The 5 panels A, B, C, D and E represent the Normal shot (−5 m), Inline shot (23 m), Midpoint shot (47 m), Inline shot (71 m) and Reverse shot (99 m) simultaneously.

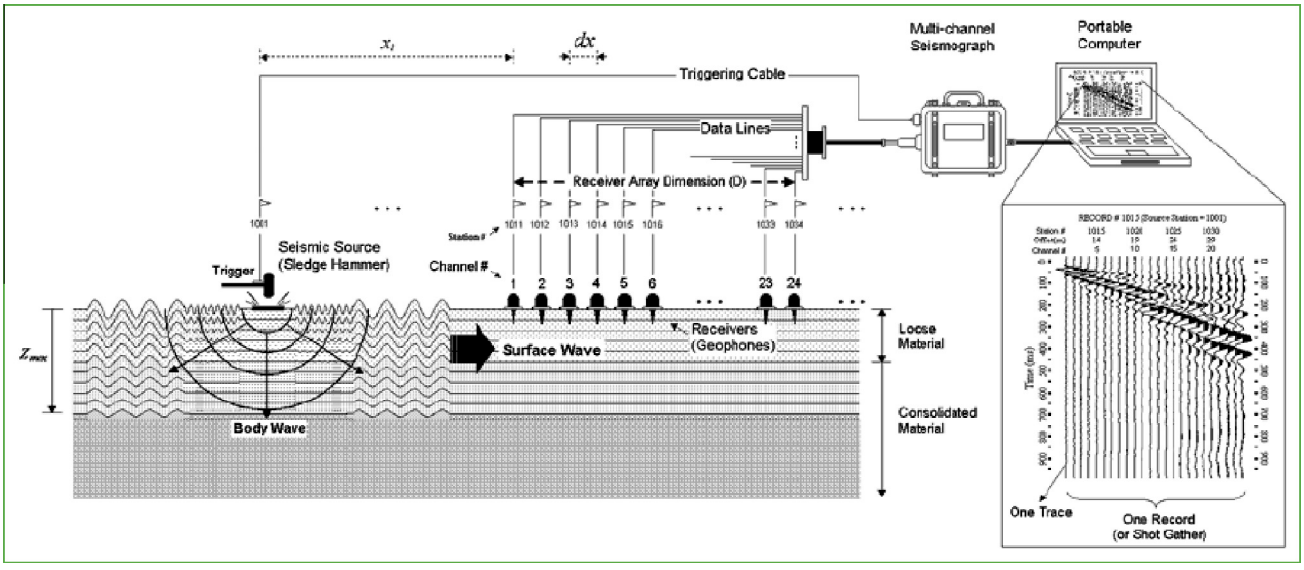

Fig. 5 The Multi channel analysis of surface waves (MASW) data acquisition configuration for determining the 1-D and 2-D shear wave velocities.

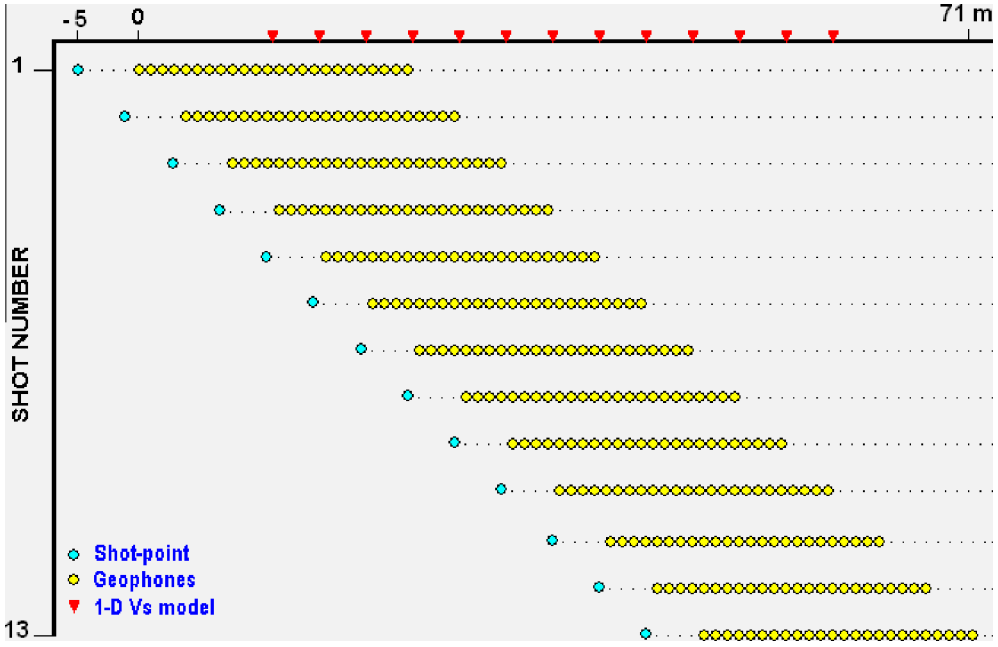

Fig. 6 Standard roll along of 2D MASW field work technique.

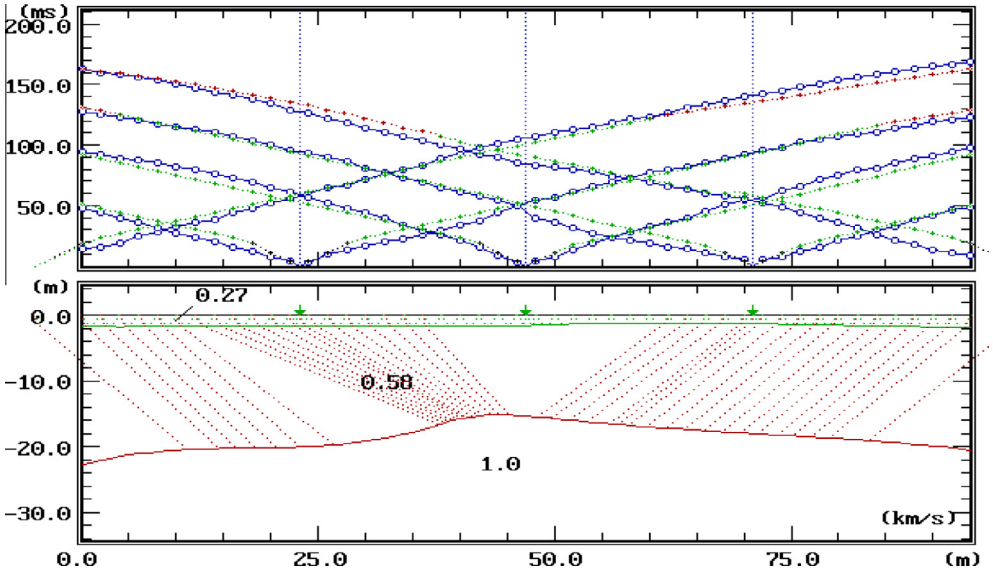

Fig. 7 The T–D curves of the five P-wave shootings (upper panel) and the 2-D depth model which consists of four layers with the corresponding P-wave velocities at the seismic profile R2C2.

(II) Pre-processing data inspection for the removal of bad records/traces.
(III) Examination for the consistence of surface wave alignment with neighboring shot gather records.
(IV) There are several factors that interfere and disturb analysis, as body waves and higher mode surface waves. These noise sources can be controlled to a limited extent during the data acquisition, but cannot be eliminated totally. Dominance of these types of noises is common with farther offset distance between the source and receiver. The above noises need to be identified and eliminated through filtering and muting (Fig. 8).
(V) Preliminary processing to assess the optimum ranges of frequency and phase velocity.

Later, the data were subjected to analyzing the overtone image of each shot gather, which represents the phase velocity versus frequency. The fundamental mode of the surface wave is the input signal used for the analysis. Accurate shear wave velocity (*Vs*) solely depends on the generation of a high quality dispersion curve, which is one of the most critical steps encountered during processing of the surface wave data, because the dispersion curve has the greatest influence in the confidence of the *Vs* profile. The dispersion program starts with

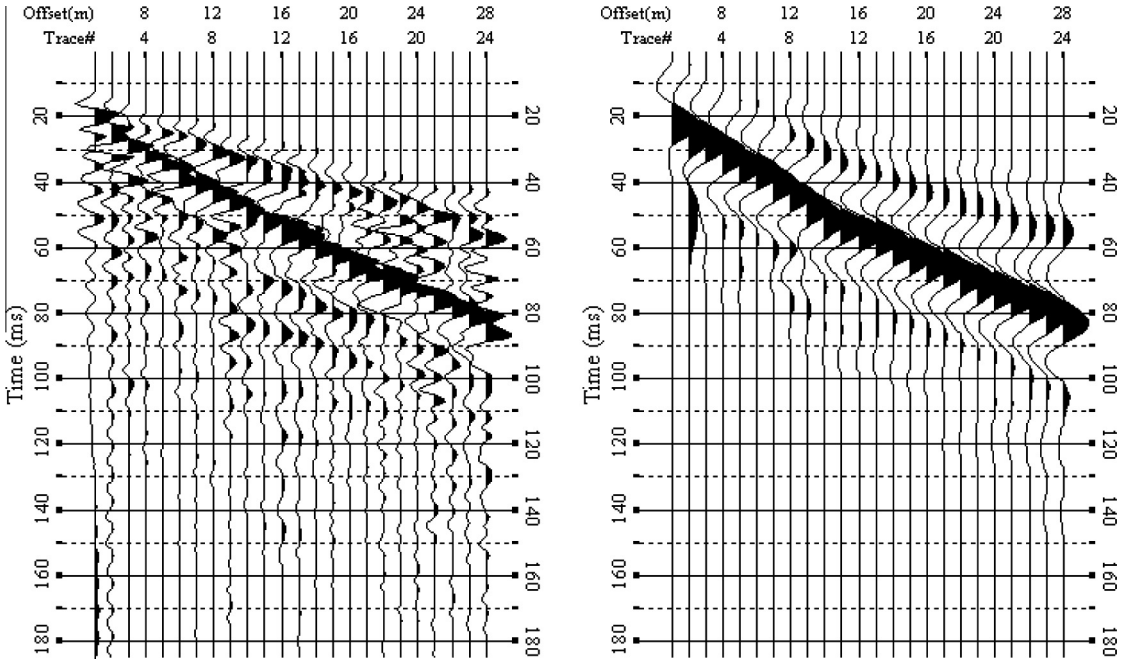

Fig. 8 The raw data of the surface-waves seismogram records (left panel) after applying the frequency filtering (right panel) of the seismic profile R2C2.

the calculation of the phase velocities within the specified frequency range. This calculation can be run several times using different values and sets of input parameters, examining the output curves until an optimum solution is identified. In general, the curve with the highest signal-to-noise ratio (S/N) represents the best choice. The estimated *Vs* section shows high S/N, indicating high confidence in the obtained phase velocity–frequency curve (Fig. 9).

Each dispersion curve is individually inverted to generate a 1D shear-wave velocity profile. The inversion uses the dispersion curve, as the only empirical data with no reference to the original seismic record. The inversion program run starts by searching for a *Vs* profile, whose theoretical dispersion curve matches with the experimental dispersion curve obtained from the dispersion analysis. The match will be evaluated on the root–mean square error (RMSE) between the two curves. The inversion algorithm first calculates the theoretical curve, using the initial *Vs* profile, then compares the theoretical curve with the experimental curve (from the RMSE perspective). If this RMSE is greater than the minimum RMSE ($E_{\min}$) specified in the control parameters, the inversion algorithm will automatically modify the *Vs* profile and repeat the procedure by calculating a new theoretical curve. Each round of this searching procedure is called iteration, and iterations continue until either the $E_{\min}$ or the maximum number of iterations (I_{MAX}) is reached. These 1D profiles appear to be the most

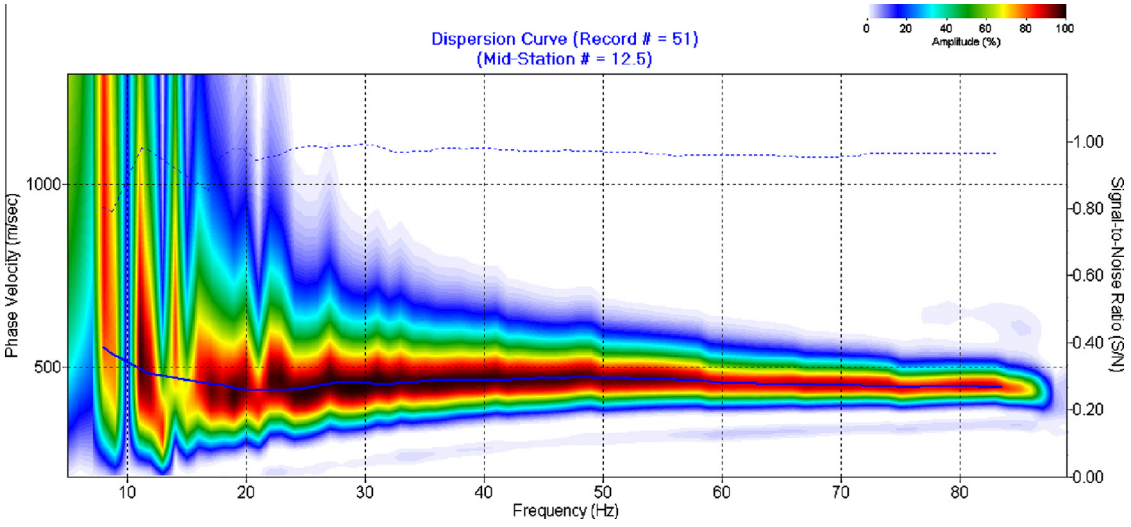

Fig. 9 The dispersion image (overtone) and the dispersion curve (phase velocity versus frequency) deduced from the surface wave records at profile R2C2, where the fundamental mode is quite clear.

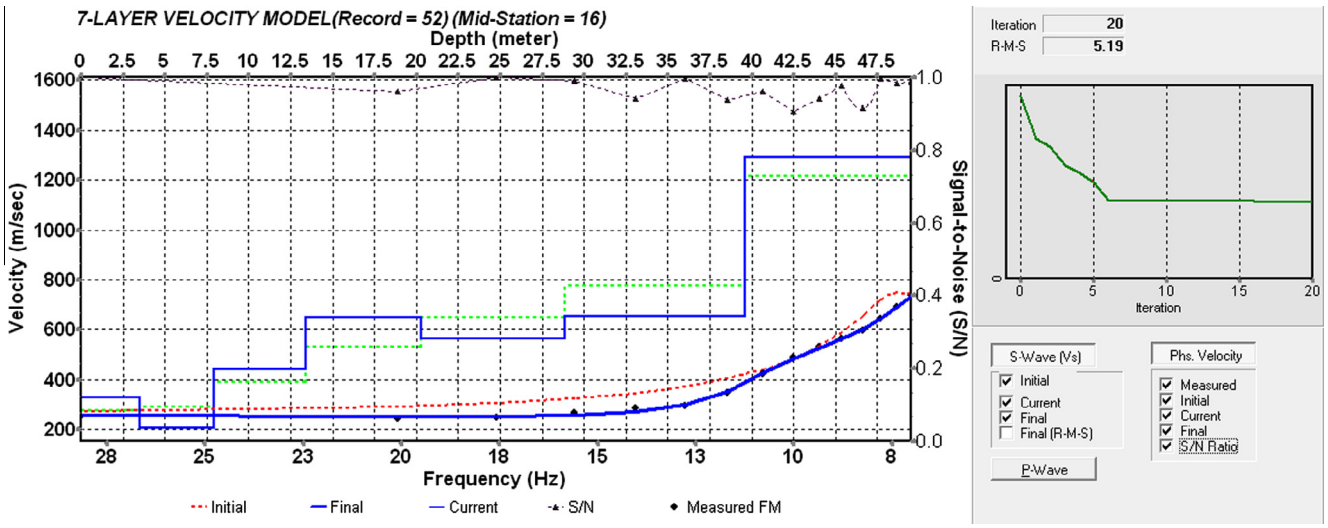

Fig. 10 The 1-D shear wave velocity profile, deduced from the inversion technique.

representative of the material directly below the middle of a geophone spread (Fig. 10).

The yielded sets of 1D plot of shear-wave velocity profiles have been interpolated, in order to produce a 2D shear wave velocity section at each site. Since a shot gather was recorded for each shot station and a shear wave velocity trace was calculated for each station location, a single 2-D contour plot of the shear wave velocity field can be produced by gathering all the velocity traces into sequential orders, according to the receiver station (Fig. 11a).

The low RMSE in estimating the *Vs* at most sites suggests a high level of confidence (Fig. 11b). The RMSE is calculated based on the *Vs* profile of a layer, whose theoretical dispersion curve best matches the calculated dispersion curve, using the RMSE as a guide and a constraint. RMSE is a measure of the relative error for each layer in comparison with the

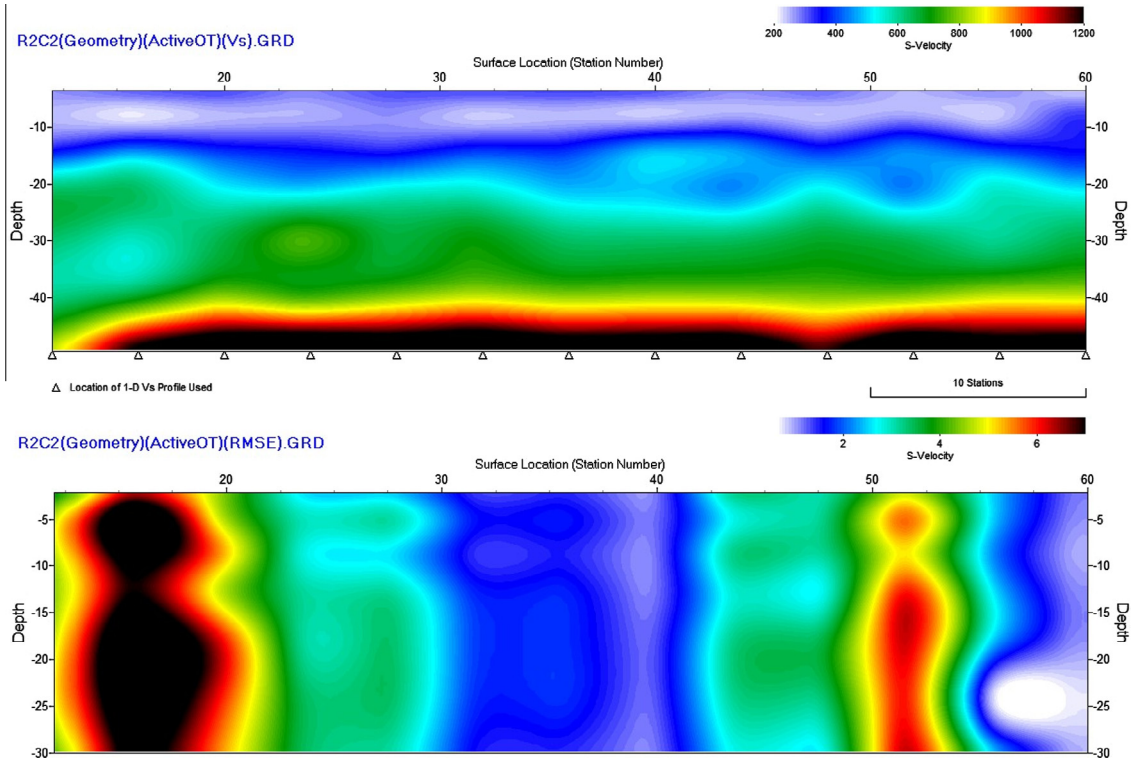

Fig. 11 The 2-D shear wave section composed of interpolation of a number of the yielded 1-D plots at R2C2 site (upper panel) and the RMSE which measure the relative error for each layer in comparison to the theoretical criteria and can be used as a measure of confidence (lower panel).

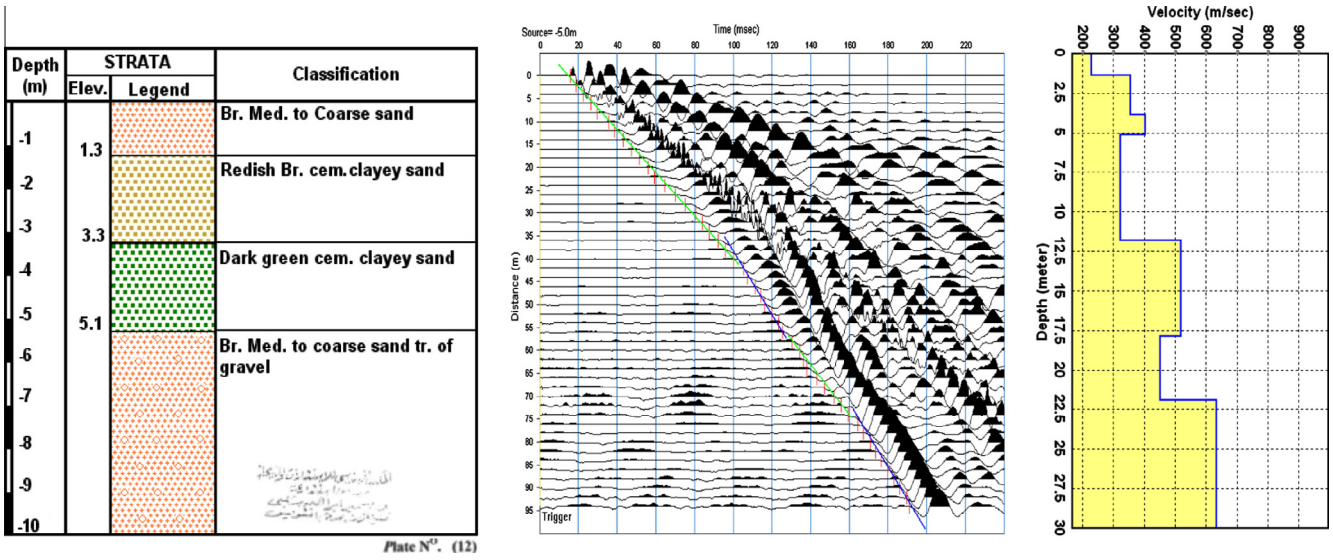

Fig. 12 The drilled borehole No. 10 (left panel), P-wave seismogram (normal shot) illustrating low velocity layer (middle panel) and the initial shear wave velocity model deduced from the borehole and P-wave seismic survey.

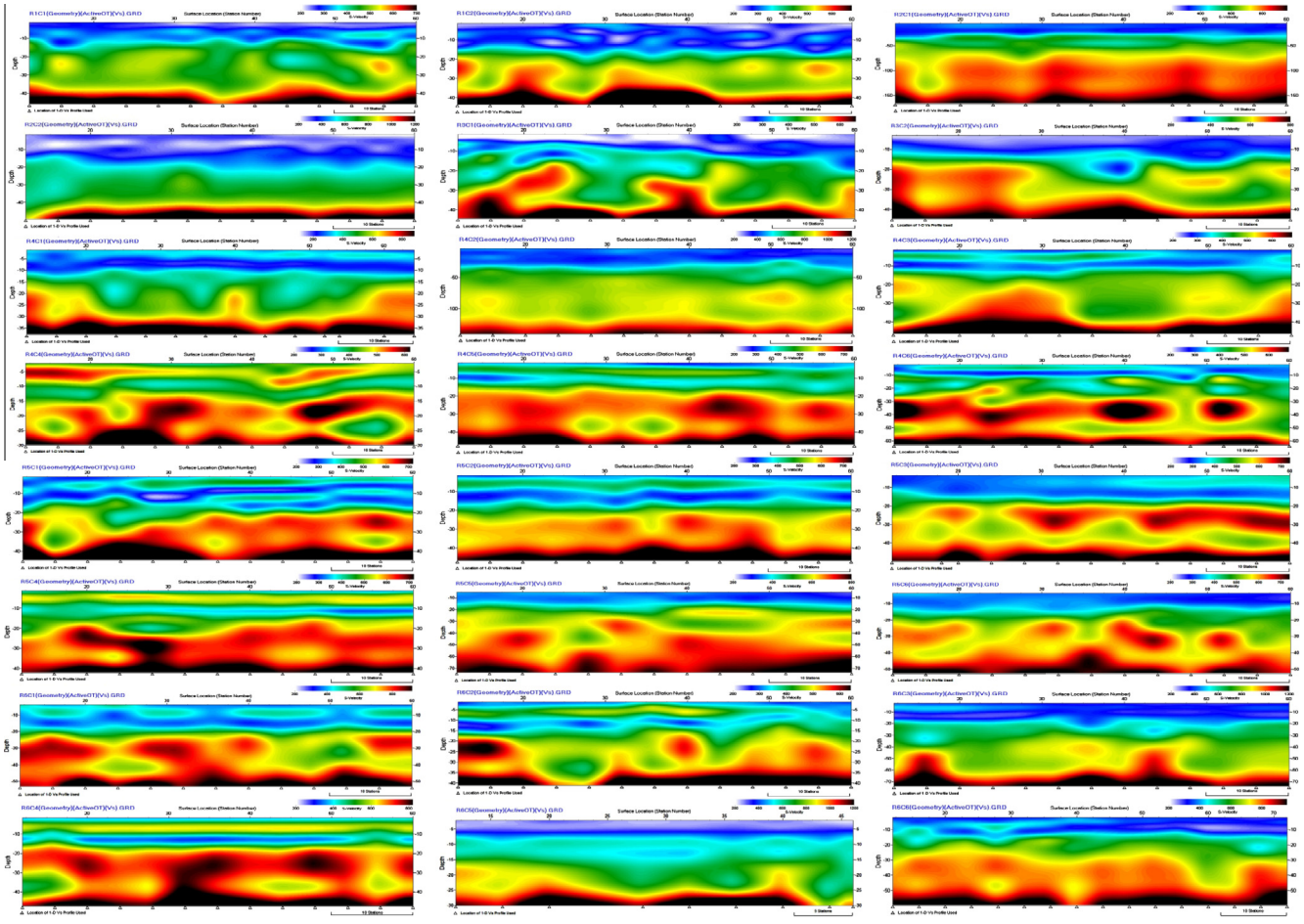

Fig. 13 The 2D shear wave velocity models at the 24 sites at the studied area.

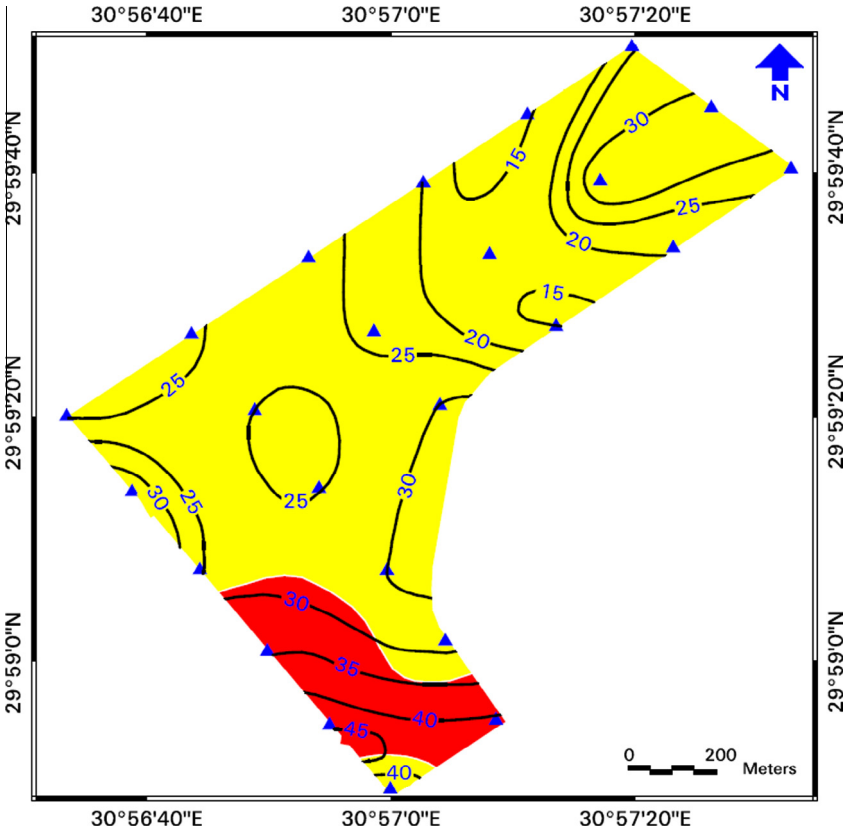

Fig. 14 The soil thickness distribution map. The yellow color represents the class C and the red color represents the D class according to the NEHRP code.

Table 1 The site classification, according to the NEHRP code.

Site Class	Average shear wave velocity V_S^{30}	Remarks
A	$V_S^{30} > 1500$ (m/s)	Hard rock
B	$760 \leqslant V_S^{30} \leqslant 1500$ (m/s)	Rock
C	$360 \leqslant V_S^{30} \leqslant 760$ (m/s)	Very dense soil or soft rock
D	$180 \leqslant V_S^{30} \leqslant 360$ (m/s)	Stiff soil
E	$V_S^{30} < 180$ (m/s)	Soil
F	$V_S^{30} < 180$ (m/s)	Soil requiring site-specific evaluation

theoretical criteria and can be used as a measure of confidence (Xia et al., 1999).

4.3. Initial shear wave profile

The geotechnical parameters of the 14 boreholes at the interested area, as shown in Fig. 3, down to a depth of 10 m, in addition to the 24 P-wave shallow seismic profiles are used to perform the initial model (initial shear wave profile). Fig. 12 illustrates the geotechnical model from the borehole, the P-wave velocity for each segment (layer) and the obtained initial shear wave profile at the site R3C2, by assuming a constant Poisson's ratio of 0.4.

5. Results

5.1. Seismic refraction and MASW

According to the first arrival P-waves picking up, the wave forms are analyzed. The deduced time distance (T–D) curves and the corresponding 2D depth models in addition to the P-wave velocity model at each profile are used to perform the initial depth models for the inversion process of the dispersion curve of the Rayleigh waves. Therefore, these measurements provide constraints for the shear wave model parameters, improving thereby the reliability of the surface wave inversion process.

The Multi-channel Analysis of Surface Waves (MASW) are recorded at 24 seismic profiles and passing the following processing steps; (i) construction of the dispersive curve (a plot of the phase velocity versus frequency), (ii) inversion of *Vs*, from the calculated dispersive curve to produce the 1D shear wave velocity model, and (iii) interpolation of the obtained 1D models to construct the 2D shear wave velocity model at each site, as shown in Fig. 13.

The 2D models demonstrate a first layer (top layer) of medium to coarse sand with *Vs* velocity in the range of 250–350 m/s and a thickness of 1–3 m. The second layer of clayey sand with a lower *Vs* velocity of about 200 m/s and a thickness of 2–4 m is shown below (Figs. 10 and 13). The third layer is of gravely coarse sand with *Vs* velocity in the range of 400–500 m/s and a thickness of 5–6 m. The fourth layer (with a

Table 2 The site classification at the studied sites, according to the NEHRP code.

Site		Coordinates (degree)		Site class	
SN	Code	Latitude	Longitude	Vs^{30} (m/s)	Class
1	R1C1	29.9804440	30.94997597	389	C
2	R1C2	29.9820366	30.95238495	354	D
3	R2C1	29.9819241	30.94859886	348	D
4	R2C2	29.9838390	30.95123672	393	C
5	R3C1	29.9836063	30.94718361	352	D
6	R3C2	29.9854431	30.94990921	396	C
7	R4C1	29.9854546	30.94564819	389	C
8	R4C2	29.9873142	30.94835854	398	C
9	R4C3	29.9892006	30.95111084	426	C
10	R4C4	29.9909973	30.95375443	484	C
11	R4C5	29.9927864	30.95641899	496	C
12	R4C6	29.9945850	30.95909691	397	C
13	R5C1	29.9872341	30.94410896	403	C
14	R5C2	29.9890823	30.94690132	422	C
15	R5C3	29.9908810	30.94961357	429	C
16	R5C4	29.9926357	30.95223999	494	C
17	R5C5	29.9943066	30.95475960	427	C
18	R5C6	29.9959793	30.95728302	417	C
19	R6C1	29.9889545	30.94261932	486	C
20	R6C2	29.9908180	30.94546318	419	C
21	R6C3	29.9925556	30.94812584	438	C
22	R6C4	29.9942627	30.95073509	548	C
23	R6C5	29.9958153	30.95310402	560	C
24	R6C6	29.9973660	30.95548248	466	C

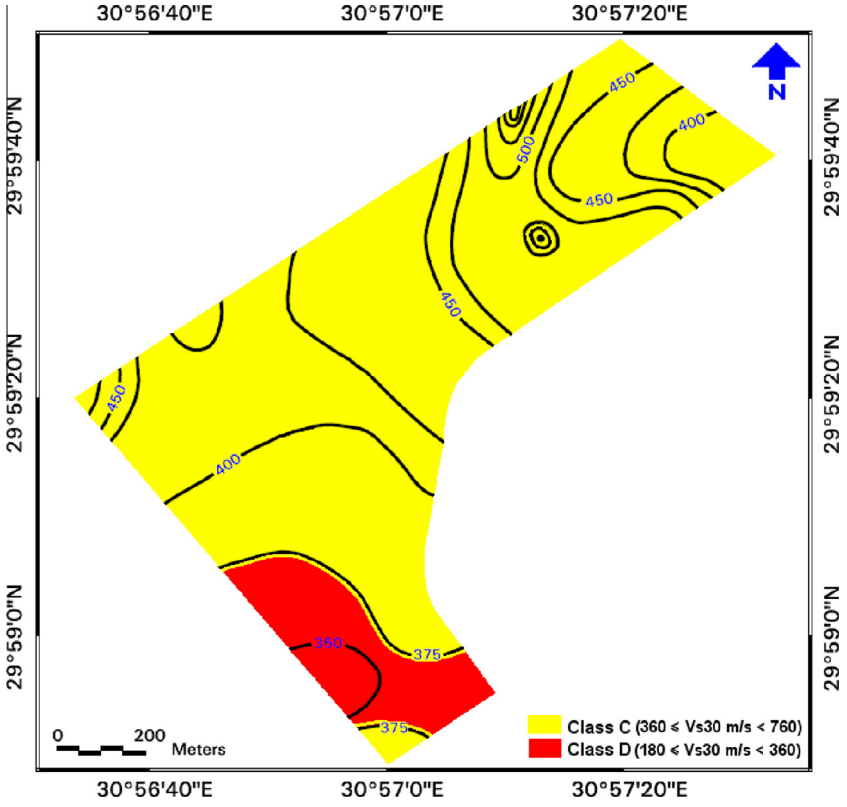

Fig. 15 The average shear wave velocity down to 30 m depth (Vs^{30}) distribution map and the site classes according to the NEHRP code.

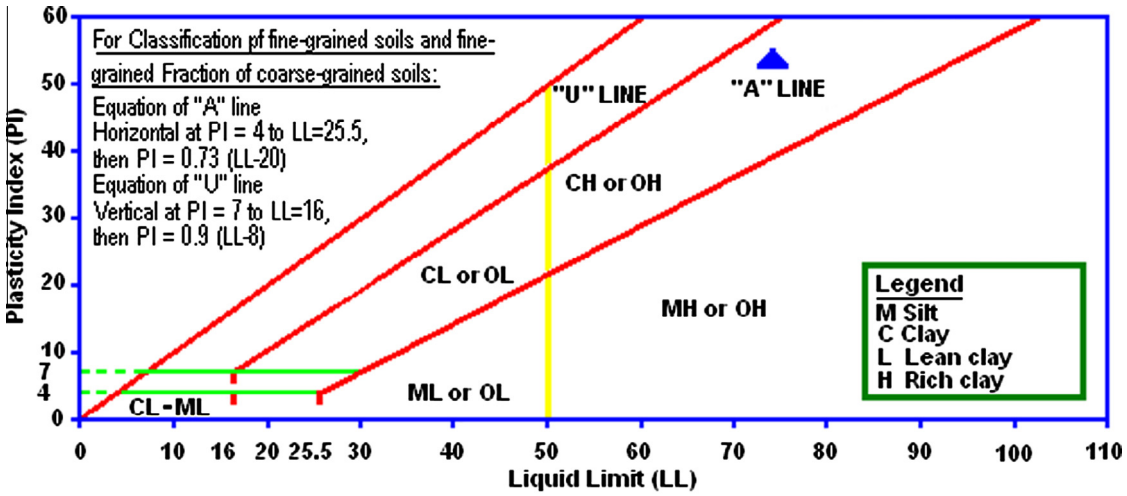

Borehole No.	Borehole depth (m)	LL	PL	PI	Sympol of Classification (USCS)
10	6	74	22	52	CH

Fig. 16 The plasticity chart test method according to ASTM D4318-05 for determining the Atterberg limits (LL, PL and PI) for the clayey sand sample.

thickness of 15–20 m and *Vs* of 650 m/s) of dense coarse sand is intercalated by a lower velocity layer of clayey sand (of thickness 6 m). The fifth layer with a high *Vs* velocity (> 1300 m/s) is assumed to be the bedrock velocity.

The depth to the engineering bedrock (*Vs* > 650 m/s) is determined in order to evaluate the soil thickness beneath each MASW profile. Fig. 14 shows the soil thickness distribution map at the studied area. The higher thickness reaches 45 m at the southern part and covered the swimming pool and some cultivated area. The lower thickness is 15 m at the eastern side, before the eastern end of the area.

5.2. Vs^{30} and site classification

The elastic properties of the near-surface materials and their effects on the seismic wave propagation are very important in earthquake geotechnical engineering, civil engineering and environmental earth science studies. The seismic site characterization for calculating the seismic hazard is usually carried out based on the near-surface shear wave velocity values. The average shear wave velocity for the depth "*d*" of the soil is referred as V_H. The average shear wave velocity down to a depth of *H* (V_H) is computed as follows:

$$V_H = \Sigma d_i / \Sigma (d_i / v_i) \quad (1)$$

where: $H = \Sigma di$ = cumulative depth in m. For the 30 m average depth, the shear wave velocity is written as:

$$Vs^{30} = \frac{30}{\sum_{i=1}^{N} (d_i / v_i)} \quad (2)$$

where: *di* and *vi* denote the thickness (in meters) and the shear-wave velocity in m/s (at a shear strain level of 10^{-5} or less) of the *i*th formation or layer respectively, in a total of N layers, existing in the top 30 m. Vs^{30} is accepted for the site classification as per NEHRP (National Earthquake Hazards Reduction Program, 2001) classification, UBC (Uniform Building Code in 1997) classification (Dobry et al., 2000 and Kanli et al., 2006) and IBC (International Building Code, 2009) classification (Table 1). In order to figure out the Vs^{30} distribution at the area under investigation, the average shear velocity has been calculated using Eq. (2) for each site. Usually, for amplification and site response studies at the uppermost 30 m, the average *Vs* is considered. However, if the rock is found within a depth of about 30 m, nearer surface shear wave velocity of the soil has to be considered. Otherwise, Vs^{30} obtained will be higher due to the velocity of the rock mass.

The Vs^{30} values for the area of interest vary between 348 m/s at site R2C1 and 560 m/s at site R6C5 (Table 2). According to the NEHRP standard, three sites (R1C2, R2C1 and R3C1) are belonging to the class D, which occupy the area of high soil thickness. While the rest sites are belonging to the category C (Fig. 15). The sites of higher velocity values are located at the lower soil thickness.

5.3. Geotechnical analysis

Soil and rock are created by many processes out of a wide variety of materials. Because deposition is most probably irregular, soils and rocks are notoriously variable and often have properties, which are undesirable from the point of view of a proposed structure. Unfortunately, the decision to develop a particular site cannot often be made on the basis of its complete suitability from the engineering viewpoint; geotechnical problems therefore occur and require geotechnical parameters for their solution.

The geotechnical information obtained from the results of the 14 drilled boreholes at the area of study (Fig. 3), as well as the field and laboratory tests and the deduced parameters from the seismic study, may reflect the behavior of the subsurface layers from the engineering point of view.

The presence of clay minerals in a fine grained soil allows it to be remolded in the presence of some moisture without

crumbling. If the clay slurry is dried, the moisture content will gradually decrease, and the slurry will pass from a liquid state to a plastic state. With further drying, it will change to a semi-solid state and finally to a solid state. These limits are the liquid, plastic and shrinkage limits. Those limits are generally referred to as the Atterberg limits. These limits were determined at the test wells and demonstrate a class of clay to rich clay (CH), according to the USCS classifications as shown in Fig. 16.

The swelling test for the claystone samples reflects its swelling ability, reaching a value of 220%. The swelling of claystone at the studied area may occur by any leakages from the drinking water, drainage and swimming pool networks.

6. Discussion

It is found that, the chance of successful survey is usually much higher with the surface wave method than with other seismic methods, particularly in detecting the near-surface anomalies and the low velocity layer. The strong nature of surface wave energy can be generated by using a simple impact source, followed by simple field logistics and processing. Most importantly, surface waves respond effectively to the various types of near-surface anomalies that are common targets of geotechnical investigations; such as the low velocity layers, caves and the near-surface structures. Continuous recording of the multichannel surface waves shows great promise in mapping the bedrock surface, delineating fracture system.... etc. Although, the surface waves are insensitive to cultural noises, they are sensitive to lateral changes in velocity.

The presence of claystone, as indicated from the drilled boreholes and low velocity layer in the 2D shear wave velocity sections, may be affected by any source of water. The swelling ability of some clay samples, which obtained from the boreholes, reaches 220%. This high swelling ratio interprets the low values of Vs^{30}, which covered the zone of class D. That zone occupies the swimming pool area and some gardens frequently subjected to water irrigation.

The higher soil thickness area reaches 45 m and covers the lower values of Vs^{30}. The lower thickness area reaches 15 m and occupies the higher values of Vs^{30}.

7. Conclusion

In order to quantify the near-surface seismic properties (P- and S-wave velocities and the dynamic elastic properties) with respect to the depth at a specific area (6th of October club), the non-invasive and low cost active seismic survey were conducted. The primary wave velocity is determined by conducting the P-wave shallow seismic refraction. The dispersive characteristics of the Rayleigh type surface waves were utilized for imaging the shallow subsurface layers by estimating the 1D (depth) and 2D (depth and surface location) shear wave velocities.

The Vs^{30} for the area of interest varies between 348 m/s at site R2C1 and 560 m/s at site R6C5. According to the NEHRP standard, three sites (R1C2, R2C1 and R3C1) are belonging to Class D, occupying the area of high soil thickness, while the rest sites are belonging to the category C. The higher the velocity sites occupy the lower soil thickness sites.

References

Anbazhagan, P., Sitharam, T., 2008. Site characterization and site response studies using shear wave velocity. J. Seismol. Earthquake Eng. 10 (2/53).

Barthelmes, A.J., 1946. Application of continuous profiling to refraction shooting. Geophysics 11, 24–42.

Baumgarte, J., 1955. Konstruktive darstellung von seismishen horizonten unter beruksichtigung der strahlen berechrung im raun. Geophys. Prospect. 3, 126–162.

Borcherdt, R.D., 1994. Estimation of site-dependant response spectra for design (methodology and justification). Earthquake Spectra 10, 617–653.

Conoco Coral, 1979. Geological map of Egypt 1:500 000. NH 36 NW Cairo.

Dobry, R., Borcherdt, R.D., Crouse, C.B., Idriss, I.M., Joyner, W.B., Martin, G.R., Power, M.S., Rinne, E.E., Seed, R.B., 2000. New site coefficients and site classification system used in recent building seismic code provisions. Earthquake Spectra 16, 41–67.

Gardner, L.W., 1939. An areal plan of mapping subsurface structure by refraction shooting. Geophysis 4, 247–259.

Gardner, G.H.F., Gardner, L.W., Gregory, A.R., 1974. Formation velocity and density – the diagnostic basics for stratigraphic traps. Geophysics 39, 770–780.

Hagedoorn, J.G., 1959. The plus-minus method of interpreting seismic refraction sections. Geophys. Prospect. 7, 158–182.

Hales, F.W., 1958. An accurate graphical method for interpreting seismic refraction lines. Geophys. Prospect. 6, 285–294.

IBC, (International Building Code) 2009. International Code Council, INC.

Kanli, A.I., Tildy, P., Pronay, Z., Pinar, A., Hemann, L., 2006. Vs^{30} mapping and soil classification for seismic site effect evaluation in Dinar region. Geophys. J. Int. SWTurkey 165, 223–235.

Louie, J.N., 2001. Faster, better: shear-wave velocity to 100 meters depth from refraction microtremor arrays. Bull. Seismol. Soc. Am. 91, 347–364.

Mahajan, Slob, Siefko, Ranjan, Rajiv, Sporry, Rob, Champati ray, P.K., van Westen, Cees J, 2007. Seismic microzonation of Dehradun city using geophysical and geotechnical characteristics in the upper 30 m of soil column. J. Seismol. 11, 355–370.

Masuda, H., 1975. Seismic refraction analysis for engineering study: OYO Technical Note. TN-10, Urawa Res., Japan.

Mohamed, A.M.E., 2009. Estimating the near surface amplification factor to minimize earthquake damage: a case study at west Wadi Hagoul area, Gulf of Suez. Egypt. J. Geophys. Prospect. 57, 1073–1089. http://dx.doi.org/10.1111/j.1365-2478.2009.00796.x.

Mohamed, A.M.E., 2003. Estimating earthquake ground motions at the Northwestern part of the Gulf of Suez. Egypt. Ph.D. Thesis, Fac. Sc., Ain Shams Uni. pp. 93–138.

Mohamed, A.M.E., Deif, A., El-Hadidy, S., Moustafa, S.S.R., El Werr, A., 2008. Definition of soil characteristics and ground response at the northwestern part of the Gulf of Suez. Egypt. J. Geophys. Eng. 5 (2008), 420–437. http://dx.doi.org/10.1088/1742-2132/5/4/006.

Nazarian, S., Stokoe II, K.H., Hudson, W.R., 1983. Use of spectral analysis of surface waves method for determination of moduli and thicknesses of pavement systems. Transp. Res. Rec. 930, 38–45.

NEHRP, 2001. NEHRP recommended provisions for seismic regulations for new buildings and other structures (FEMA 368 and 369). 2000 Building Seismic Safety Council, National Institute of Building Sciences, Washington, DC.

Palmer, D., 1980. The generalized reciprocal method of seismic refraction interpretation. Soc. Explor. Geophys..

Park, C.B., Xia, J., Miller, R.D., 1998. Imaging dispersion curves of surface waves on multichannel record. In: 68th Ann. Internat. Mtg., Soc. Expl. Geophys., Expanded Abstracts, pp. 1377–1380.

Park, C.B., Miller, R.D., Xia, J., 1999. Multichannel analysis of surface waves (MASW). Geophysics, 64.

Park, C.B., Miller, R.D., and Miura, H., 2002. Optimum field parameters of an MASW survey, [Exp. Abs.]. SEG-J, Tokyo, 22–23.

Rockwell, D.W., 1967. A general wave front method. In: Musgrave, A.W., (Ed.), Seismic Refraction Prospecting, Tulsa, Soc. Explor. Geophys. pp. 363–415.

SeisRefa, 1991. Refraction analysis program, version 1.30, USA. Copyright, Oyo Corporation.

Slotnick, M.M., 1950. A graphical method for the interpretation of refraction profile data. Geophysics 15, 163–180.

Stokoe II, K.H., Wright, G.W., James, A.B., Jose, M.R., 1994. Characterization of geotechnical sites by SASW method. In: Woods, R.D. (Ed.), Geophysical Characterization of Sites: ISSMFE Technical Committee #10. Oxford Publishers, New Delhi.

Tarrant, L.H., 1956. A rapid method of determining the form of a seismic refractor from line profile results. Geophys. Prospect. 4, 131–139.

Thornburgh, H.R., 1930. Wave front diagrams in seismic interpretation. Bull. A. A. P. G. 14, 185–200.

Tian, G., Steeples, D.W., Xia, J., Miller, R.D., 2003. Multichannel analysis of surface wave method with the auto juggle. Soil Dyn. Earthquake Eng. 23, 243–247.

Xia, J., Miller, R.D., Park, C.B., 1999. Estimation of near surface shear-wave velocity by inversion of Rayleigh wave. Geophysics 64 (3), 691–700.

Xia, J., Miller, R.D., Park, C.B., Hunter, J.A., Harris, J.B., 2000. Comparing shear-wave velocity profiles from MASW with borehole measurements in unconsolidated sediments, Fraser River Delta, B.C. J. Environ. Eng. Geophys. Canada 5(3) 1–13.

Xia, J., Miller, R.D., Park, C.B., Hunter, J.A., Harris, J.B., Ivanov, J., 2002. Comparing shear-wave velocity profiles inverted from multichannel surface wave with borehole measurements. Soil Dyn. Earthquake Eng. 22, 181–190.

Zywicki, D., Rix, G.J., 1999. Frequency-wave number analysis of passive surface waves. In: Proc. Symp. on the Appl. of Geophys. to Environm. and Eng. Problems, Oakland, pp. 75–84.

Wyrobek, S.M., 1956. Application of delay and intercept times in the interpretation of multi layer refraction time distance curves. Geophys. Prospect. 4, 112–130.